Optimization and Statistical Modeling of Ultrasonic Depolymerization of κ-Carrageenan Using RSM: Predominant Role of pH, Temperature-Time Interactions, and Mechanistic Insights

Nita Indriyani [a,1,*], Puji Rahayu [b,2], Ummu Musfika [a,3], Dewi Sri Ayuningsih [a,4]

[a] Department of Chemical Engineering, Faculty of Engineering, Universitas Pendidikan Muhammadiyah Sorong, Southwest Papua, Indonesia
[b] Department of Petrochemical Industrial Process Technology, Banten Petrochemical Industry Polytechnic Department, Banten, Indonesia
[1] nitaindriyani@unimudasorong.ac.id *; [2] puji.rahayu@poltek-petrokimia.ac.id; [3] ummumusfika@unimudasorong.ac.id;
[4] dewisriayungsih@unimudasorong.ac.id
* corresponding author

ARTICLE INFO

Article history
Received September 3, 2025
Revised September 26, 2025
Accepted September 26, 2025

Keywords
Carrageenan
Depolymerization
Molecular weight
Response Surface Methodology
Ultrasonic

ABSTRACT

κ-carrageenan is a sulfated polysaccharide from red seaweed widely used in the food and pharmaceutical industries. In its low-molecular-weight form (<20 kDa), it exhibits improved cellular uptake and more potent biological activity, making it highly attractive for biomedical applications. Ultrasonic-assisted depolymerization provides an effective method for reducing molecular weight while preserving functional sulfate groups. This study statistically modeled the effects of temperature, time, and pH on κ-carrageenan depolymerization using Response Surface Methodology (RSM) with a Central Composite Design (CCD). Experiments were conducted at temperatures ranging from 40 to 60°C, with sonication times of 16 to 32 minutes, and at pH levels of 3 and 6. Molecular weight was estimated via intrinsic viscosity, and structural changes were analyzed by FTIR spectroscopy. The results showed that pH was the most influential factor, with acidic conditions (pH 3) promoting greater molecular weight reduction than near-neutral conditions (pH 6). Temperature and time also had significant effects, and the RSM model effectively captured both linear and quadratic interactions. ANOVA confirmed the model's reliability, with high coefficients of determination (R^2 = 0.9684 at pH 3 and R^2 = 0.9712 at pH 6). FTIR analysis revealed cleavage of α(1→3) and β(1→4) glycosidic bonds, while sulfate ester groups remained stable. In conclusion, ultrasonic depolymerization coupled with RSM provides a predictive and reliable framework to optimize low-molecular-weight κ-carrageenan production for biomedical applications.

1. Introduction

Seaweed can be classified based on the chemical compounds it contains, thus recognizing carrageenan-producing seaweed (carrageenophytes), agar (agarophytes), and alginate (alginophytes). Based on this classification, red algae (Rhodophyceae) such as Euchema spinosum and Euchema cottoni are classified as carrageenan-producing seaweed because they have high carrageenan content, around 62-68% of their dry weight [1], [2]. Carrageenan is composed of repeating galactose and 3,6-anhydrogalactose (3,6-AG) units. Both, whether sulfate-linked or not, are linked by alternating α–1,3 and β–β-1,4 glycosidic bonds [3], [4], [5].

Euchema cottoni is a type of red seaweed that changed its name to Kappaphycus alvarezii because the carrageenan produced includes the kappa-carrageenan fraction. Kappa-carrageenan (K-carrageenan) is composed of α(1,3)-D-galactose-4-sulfate and β(1,4)-3,6-anhydro-D-galactose and

contains D-galactose-6-sulfate ester and 3,6-anhydro-D-galactose-2-sulfate ester [3], [6], [7]. K-carrageenan has begun to be developed in biomedical applications as a tumor growth inhibitor [8], antiviral [9], [10], anticoagulant [11], and antioxidant [12]. K-carrageenan that is useful in biomedical applications is low molecular weight κ-carrageenan, which has a molecular weight of <20 kDa [12]. This is because κ-carrageenan can enter cells more efficiently and effectively than high-molecular-weight carrageenan [13]. The negative charge of low-molecular-weight κ-carrageenan will provide an inhibitory effect that interacts with the positive charge of the virus or cell surface, subsequently preventing the virus from penetrating the cell [14], [15].

One technique to reduce the molecular weight of κ-carrageenan is the depolymerization process using ultrasonic irradiation, which utilizes ultrasonic waves to produce cavitation bubbles that break the polymer chain [16], [17]. The depolymerization process is influenced by process parameters such as temperature, time, and solution pH [18], [19]. Variations in these three parameters can result in significant differences in the molecular weight distribution; therefore, controlling the process conditions is a crucial factor in obtaining accurate results. Studies that systematically integrate the effects of temperature, time, and pH parameters on changes in the molecular weight of carrageenan are still limited. A previous study, entitled "Kinetics and thermodynamics of ultrasound-assisted depolymerization of κ-carrageenan," reported that temperature and time affect the Kinetics and thermodynamics of ultrasonic-assisted κ-carrageenan depolymerization, using a pseudo-first-order kinetic model [17]. However, the pH variable has not been considered, so the description of the reaction environment's effect remains limited. Another study, which included pH variations in addition to temperature and time, entitled "The Kinetics And Thermodynamics Study Of Ultrasound-Assisted Depolymerization Of K-Carrageenan In Acidic Solution", also provided more comprehensive information regarding the acid mechanism in the depolymerization process [18]. However, these two studies analyzed the influence of factors partially. They did not account for interactive effects (e.g., temperature–pH, time–pH) or quadratic impacts that can only be captured by a multivariate approach, such as Response Surface Methodology (RSM).

RSM is a statistical technique for analyzing and optimizing the relationship between several factors (input variables) and responses (output variables) [20], [21]. RSM was introduced in the 1950s and has since been widely applied in various fields, including the chemical and process industry, food science, pharmaceutical formulation, and environmental chemistry [20], [22], [23]. Generally, RSM is used to identify optimal points in a process or system and to investigate and understand the effects of interactions between various components [24]. The central composite design (CCD) model is one of the RSM methods, namely the design of a response surface that provides information about the influence of experimental variables and overall experimental error in a minimum number of trials [25], [26], [27]. RSM is carried out by creating a model and analyzing the response Y, which is influenced by the variable X. The relationship between the response Y and the independent variable X [27] is:

$$Y= f(X_1, X_2,\ldots, X^k) + \varepsilon^i = 1,2,3, .k \quad (1)$$

$$Y=\beta_0+\sum\beta_i X_{iki=1}+\sum\beta_{iiki=1}X_{i2}+\sum\sum_{i<j}X_iX_j+\varepsilon \quad (2)$$

where: Y: observed response; β_0: regression parameter; X_i: linear principal variable; X_iX_j: two-variable linear; X_i^2: quadratic principal variable.

Therefore, this study was conducted to fill this gap in previous research by developing an RSM-based predictive model that examines not only the main effects but also the complex and non-linear interactions between parameters. This approach was used to quantitatively analyze the molecular weight reduction of κ-carrageenan through ultrasonic depolymerization, thereby providing a more accurate description of the optimum conditions than previous methods. Furthermore, the developed quadratic model can illustrate the presence of a non-linear optimum response, which is essential for predicting the best operating conditions.

2. Research Methodology

2.1. Materials

The materials used in this study were κ-carrageenan derived from the seaweed Kappaphycus alvarezii, produced by CV (water content of less than 12%), 37% hydrochloric acid (HCl) (E. Merck

Cat. No. 100314), distilled water, and isopropyl alcohol (E. Merck Cat. No. 818766). The equipment used included a Krisbow KLS 303365 ultrasonic batch apparatus (40kHz, 35W, 110V, 0.8 L), a batch heater, a Ubbelohde-type capillary viscometer, and a thermometer.

2.2. Procedures

This study began with the preparation of carrageenan raw materials to remove impurities. The preparation process included dissolution at 70°C, followed by purification and flocculation. Next, drying and grinding were performed to obtain a pure carrageenan powder. The depolymerization process is referred to in previous research [18]. Pure carrageenan powder was dissolved in 0.5% w/v Aquadest and then degraded/depolymerized using ultrasonic irradiation. Temperature and time parameters were varied during the ultrasonic degradation process, and pH conditions were adjusted with HCl solution. After that, the viscosity of the depolymerization results was measured using a Ubbelohde-type capillary viscometer. The design of the experimental data using the Central Composite Design (CCD) is presented in the Table, while the process flow is presented in Fig. 1.

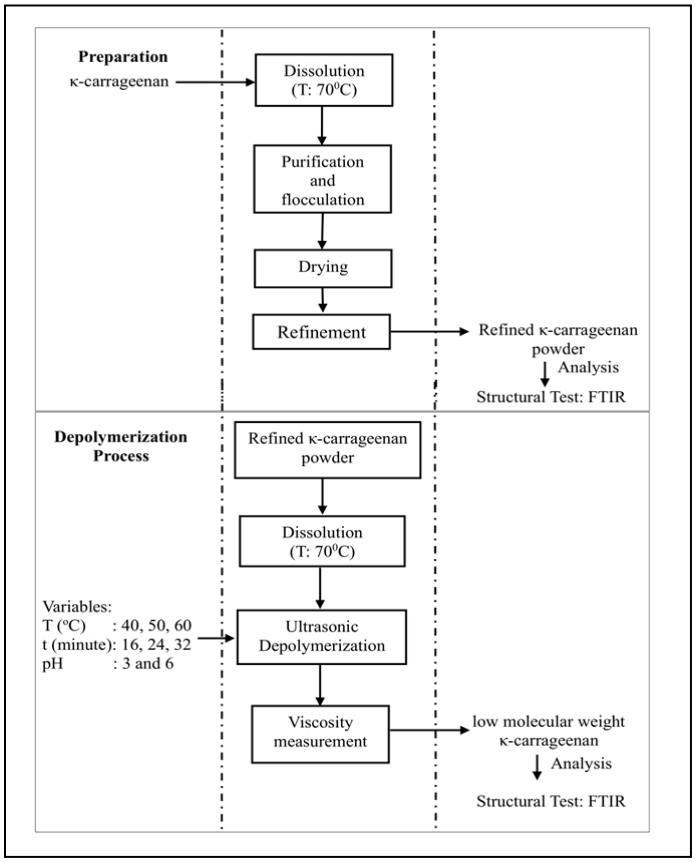

Fig. 1. Depolymerization Process Diagram

Table 1. Experimental Data Design with CCD

Run	Coded		Independent variables	
	X_1	X_2	X_1 (T, °C)	X_2 (t, minute)
1	-1	-1	40.0	16.0
2	-1	1	40.0	32.0
3	1	-1	60.0	16.0
4	1	1	60.0	32.0
5	-α	0	35.9	24.0
6	+α	0	64.1	24.0
7	0	-α	50.0	12.7
8	0	+α	50.0	35.3
9	0	0	50.0	24.0
10	0	0	50.0	24.0

2.3. Molecular Weight Calculation

The molecular weight of carrageenan is calculated based on intrinsic viscosity. Intrinsic viscosity is obtained from specific viscosity using the Huggins Equation [28].

$$[\eta_{sp}/C] = [\eta] + kH\,[\eta]^2\,C \quad (3)$$

Where, η_{sp} is the specific viscosity; C is the solution concentration (g/ml); kH is the Huggins constant (0.3); [η] is the intrinsic viscosity (ml/g). Once the inherent viscosity is obtained, the molecular weight of carrageenan can be calculated using the Mark-Houwink equation [28].

$$[\eta] = k_{MH}.\,M^a \quad (4)$$

$$M = ([\eta]/k_{MH})^{1/a} \quad (5)$$

Where k_{MH} and a are constants for the known system; M is the molecular weight (kDa). In previous studies, the k_{MH} value was 0.00778, and for carrageenan was 0.90 [28], [29].

3. Results and Discussion

3.1. Experimental Data Analysis and the Influence of Variables

The experimental design employed the CCD method, which was conducted 10 times with two selected independent variables: temperature (X_1) and time (X_2). The experimental data obtained were used to calculate the coefficients of the polynomial equation [30]. Furthermore, the data were analyzed using RSM to understand the effect of independent variables on the molecular weight of the depolymerization product at different pH conditions. Table 2 presents the results of the depolymerization experiment.

Table 2. Experimental Data of Depolymerization with CCD

Run	Coded		Independent variables		Dependent variables (Molecular weight, kDa)			
	X_1	*X_2*	*X_1 (T, °C)*	*X_2 (t, minute)*	*Actual*	*Prediction*	*Actual*	*Prediction*
1	-1	-1	40.0	16.0	443	472	187	192
2	-1	1	40.0	32.0	282	296	108	97
3	1	-1	60.0	16.0	259	255	73	92
4	1	1	60.0	32.0	107	78	15	17
5	-α	0	35.9	24.0	527	498	146	151
6	+α	0	64.1	24.0	166	190	37	24
7	0	-α	50.0	12.7	402	331	187	172
8	0	+α	50.0	35.3	123	81	44	51
9	0	0	50.0	24.0	153	206	98	97
10	0	0	50.0	24.0	151	206	97	97

Table 2 shows 10 systematically designed runs. Analyzable patterns include:

1) Variation based on experimental design

Runs 1-4 are a 22-factorial design, namely (-1,1), (-1,1), (1,-1), and (1,1), which tests the combined effects of temperature and time at the corner points of the design. Runs 5-8 are axial points or star points, namely (-α,0), (+α,0), (0,-α), and (0,+α). These points help in estimating the curvature of the response. Runs 5-6 tests to examine the effect of temperature at extreme values (-α and +α) when time is set at the midpoint (24 minutes). Runs 9-10 are repeated at the midpoint (0,0). This repetition is crucial for measuring experimental error and testing the model's curvature. The obtained values (153 and 151) indicate that the variation between experiments at the midpoint is relatively small, indicating good precision.

2) Effect of Independent Variables on Molecular Weight.

The effect of temperature (X_1) shows that increasing temperature tends to decrease molecular weight, as evidenced by comparing runs at the same time but at different temperatures. For example, runs 1 (40°C) and 3 (60°C) took 16 minutes, runs 2 (40°C) and 4 (40°C) took 32 minutes, and runs 5 (35.9°C) and 6 (64.1°C) took 24 minutes. The same pattern occurred at both pH conditions. Run 4 (high temperature, long time) produced the lowest molecular weight, namely 107 kDa at pH 6 and

15 kDa at pH 3. This suggests that the combined effect of these two variables is strong, influencing polymer breakdown.

3) Effect of pH Conditions

More acidic conditions (pH 3) yielded a significantly lower molecular weight than those at pH 6, as observed in run 4. This indicates that the depolymerization process is more effective and faster in an acidic environment.

4) Model Accuracy

In general, the predicted values were quite close to the actual values. For example, at pH 6, run 1, the exact value was 443 kDa, while the expected value was 488 kDa. At pH 3, run 1, the actual value was 187 kDa, while the expected value was 192 kDa. This indicates that the regression model created from these data has good accuracy in predicting molecular weight based on variations in temperature and time. However, there were slightly larger differences between the actual and predicted values in some runs, such as in runs 5 and 7 at pH 6. This is normal and can be further explained by statistical analysis, such as the R-squared or p-value of the model.

The temperature and time parameters in Table 2 show that both affect molecular weight. Increased temperature and time indicate degradation or depolymerisation of the molecular chain, resulting in a reduction of the molecular weight. The most crucial factor in Table 2 above is the pH condition. The pH condition of 3 drastically accelerates the process of depolymerisation of the molecular chain compared to pH 6. Strong acidic conditions (pH 3) result in a higher concentration of protons (H^+) compared to pH 6, allowing protons to easily attack oxygen in glycosidic bonds, which causes bond cleavage [17], [18], [31].

3.2. Simultaneous Regression Coefficient Test with ANOVA

An ANOVA test was conducted on the experimental data to understand the equation model that connects the independent variables to the response and to determine the significance of the independent variables. The results of the ANOVA test are presented in Table 3.

Table 3. ANOVA Test on the Molecular Weight of Kappa Carrageenan Depolymerization

Factors	df	Adj SS	Adj MS	F-Value	F-Table	P-Value
pH 3						
Linear						
X_1	1	16279.62	16279.62	63.3	7.19	0.001352
X_2	1	14519.74	14519.74	56.45	7.19	0.001679
Quadratic						
X_1	1	114.20	114.20	0.44	7.19	0.541642
X_2	1	230.41	230.41	0.89	7.19	0.397482
Interaction						
X_1X_2	1	107.12	107.12	0.41	7.19	0.553830
Error	4	1028.72	257.18			
Lack of Fit	3	1008.72	336.24	16.65		
Pure Error	1	20	20			
		R^2=0.9684 dan R^2 adjusted 0.9288				
pH 6						
Linear						
X_1	1	94725.9	94725.9	65.7	7.19	0.001259
X_2	1	62501.1	62501.1	43.35	7.19	0.002755
Quadratic						
X_1	1	36402.4	36402.4	25.3	7.19	0.007332
X_2	1	10283.4	10283.4	7.13	7.19	0.055768
Interaction						
X_1X_2	1	20.2	20.2	0.01	7.19	0.911375
Error	4	5767.4	1441.85			
Lack of Fit	3	5427.4	1809.13	5.3		
Pure Error	1	340	340			
		R^2=0.9712 dan R^2 adjusted 0.9351				

Table 3 presents the ANOVA results for two different pH conditions (pH 3 and pH 6). The analysis was to determine which factors (X_1 and X_2) significantly influence the response and the interactions between these factors. This analysis considered the linear, quadratic, and interaction effects of the factors. The excellent ability to explain data variation is evident from the high R^2 values at each pH, specifically pH 3 ($R^2 = 0.9684$) and pH 6 ($R^2 = 0.9712$). The R^2 values indicate a high model fit, and the factors can explain the response.

Linear factors X_1 and X_2 had a significant influence on the response at both pH values (p-value < 0.05). The high F-values (63.3 and 56.45 at pH 3; 65.7 and 43.35 at pH 6) confirmed the strong influence of X_1 and X_2. Conversely, the interaction between X_1 and X_2 (X_1X_2) showed no significant effect at both pH values because the p-value was >0.05, indicating that X_1's impact on the response was independent of the level of X_2. The fundamental difference between the two models lies in the significance of the quadratic effect. At pH 3, the quadratic effect was insignificant for both X_1 and X_2 because the p-value was >0.05. This indicates a linear relationship between the factors and the response. The response surface under these conditions can be depicted as a plane, Fig. 2. (a), meaning that changes in the reaction are proportional to changes in X_1 and X_2. At pH 6, a significant quadratic effect was observed for X1 (p-value < 0.05), whereas for X2, the effect was insignificant. This indicates that the relationship between X_1 and the response is non-linear or curvilinear. The response surface at this condition has significant curvature along the X_1 axis, Fig. 2. (b).

3.3. Individual Regression Coefficient Test and Mathematical Model

Individual coefficient testing was performed using the same α value, namely α = 0.05 or 5%. The results of the particular regression coefficient testing are presented in Table 4.

Table 4. Estimated Values of Individual Regression Coefficients

Factors	Reg. Coeff	SE. Coeff	T	P
pH 3				
Model	97.4350	11.3398	8.5923	0.0010
X_1	-45.1104	5.6699	-7.9562	0.0014
X_2	-42.6024	5.6699	-7.5138	0.0017
X_1^2	-4.9981	7.5005	-0.6664	0.5416
X_2^2	7.0994	7.5005	0.9465	0.3975
X_1X_2	5.1750	8.0184	0.6454	0.5538
pH 6				
Model	151.9350	26.8493	5.6588	0.0048
X_1	-108.8151	13.4247	-8.1056	0.0013
X_2	-88.3891	13.4247	-6.5841	0.0028
X_1^2	89.3338	17.7592	5.0303	0.0073
X_2^2	47.4288	17.7592	2.6707	0.0558
X_1X_2	2.2500	18.9854	0.1185	0.9114

Individual regression coefficients with a probability value greater than α (α = 0.05) will be removed as they have no significant effect. The results of the new regression coefficients for molecular weight after removing insignificant coefficients are presented in Table 5.

Table 5. Estimated Regression Coefficient Values

Factors	Reg. Coeff	SE. Coeff	T	P
pH 3				
Model	99.1160	4.968912	19.94722	0.000000
X_1	-45.1104	5.555413	-8.12009	0.000083
X_2	-42.6024	5.555413	-7.66864	0.000119
pH 6				
Model	206.139	23.95734	8.60443	0.000136
X_1	-108.815	18.29772	-5.94692	0.001011
X_2	69.007	21.86996	3.15534	0.019681
X_1^2	-88.389	18.29772	-4.83061	0.002908

The variables temperature and time showed dominant significance with T-values of 7.41214 and 4.26130, respectively. Thus, changes in temperature and time will affect the response, namely, the molecular weight at pH 3 and pH 6.

After conducting a regression coefficient test on the molecular weight response, a mathematical model that shows the influence of independent variables such as temperature (X_1) and time (X2) on the molecular weight response, the mathematical model can be determined as follows:

pH 3: $$Y= 99.116 – 45.1104\ X_1 – 42.6024\ X_2 \quad (5)$$

pH 6: $$Y= 206.139 – 108.815\ X_1 + 69.007\ X_2 – 88.389\ X_1^2 \quad (6)$$

The Y code represents the response, specifically the molecular weight, while X_1 and X_2 denote temperature and time, respectively. Based on the regression equation obtained, it can be seen that at pH 3, the X_1 and X_2 values have a significant and linear adverse effect on the molecular weight response. At pH 6, the relationship appears more complex. The X_1 value exhibits a non-linear effect, as indicated by the significant coefficient X_{12}, whereas X_2 has a considerable positive impact (in contrast to pH 3). The two regression equations above suggest that the effect of X_1 and X_2 on Y is not constant, but rather depends on the pH conditions.

At pH 6, the regression coefficient for the time variable (X_2) is positive, indicating that increasing the sonication time does not always result in a decrease in molecular weight, and may even lead to an increase. This can be explained by differences in depolymerization mechanisms, which are influenced by pH. Previous research reported that at low pH (pH 3), κ-carrageenan depolymerization is controlled by acid hydrolysis with an activation enthalpy ($\Delta H‡$) of 29.99 $kJ \cdot mol^{-1}$, so that the longer the sonication, the more consistent the decrease in molecular weight. Conversely, at pH 6, the $\Delta H‡$ value is lower (15.56 $kJ \cdot mol^{-1}$), indicating a lower activation energy but also a decreased effectiveness of chain cleavage [18]. Under these conditions, the dominant mechanisms shift to cavitation collapse and the formation of oxidative radicals (•OH, H_2O_2), which are less linear with time because, after initial fragmentation, reorganization or even recombination between fragments can occur. This non-linear phenomenon aligns with previous research findings, which show that the ultrasonic degradation of polyacrylamide occurs rapidly at the beginning, then approaches a limiting molecular weight, making additional time no longer adequate, and sometimes giving the impression of an increase in molecular weight [32]. Other studies have also reported that ultrasonic degradation can produce initial fragmentation followed by conformational changes and possible secondary aggregation, so the response to time is not always a linear decrease [16]. Furthermore, literature related to acid and ultrasonic hydrolysis supports these findings, explaining that at low pH, acid hydrolysis can accelerate the cleavage of glycosidic bonds intensely but tends to be uncontrolled, producing tiny, less stable fragments [33]. Conversely, at intermediate pH values, such as pH 6, hydrolysis is more selective, resulting in a more uniform and stable molecular weight distribution.

Meanwhile, other studies confirm that ultrasonic cavitation primarily works through shear forces that weaken glycosidic bonds and damage non-covalent bonds [34]. At intermediate pH conditions, cavitation attacks are more effective because they do not compete excessively with protonation, allowing for a more controlled reduction in molecular weight. Thus, the positive X_2 value at pH 6 can be understood as the result of an interaction between the physical-radical mechanism resulting from ultrasonic cavitation and the more moderate acid hydrolysis mechanism. This finding reinforces the importance of multivariate analyses, such as RSM, as they can capture complex interactions between parameters that a single-factor-at-a-time approach cannot explain.

3.4. Response Surface Plots

The experimental data in Table 2 can be visualized using a response surface graph Fig. 2. This graph illustrates the relationship between molecular weight (Z-axis), temperature (X-axis), and time (Y-axis) variations, thereby providing a more precise identification of patterns and trends. Fig.2. illustrates the surface response to pH 3 and pH 6. The surface response plot in Fig. 2. (a) at pH 3 shows a relatively flat or sloping surface resembling a plane. This shape visually confirms the absence of a significant quadratic effect. The pH 3 condition also results in a significantly lower molecular weight, with a color scale ranging from 0 to 300 kDa. The surface response plot in Fig. 2(b) displays a distinctly concave, or bowl-shaped, surface. This shape visually confirms the ANOVA findings, namely a significant quadratic effect of temperature.

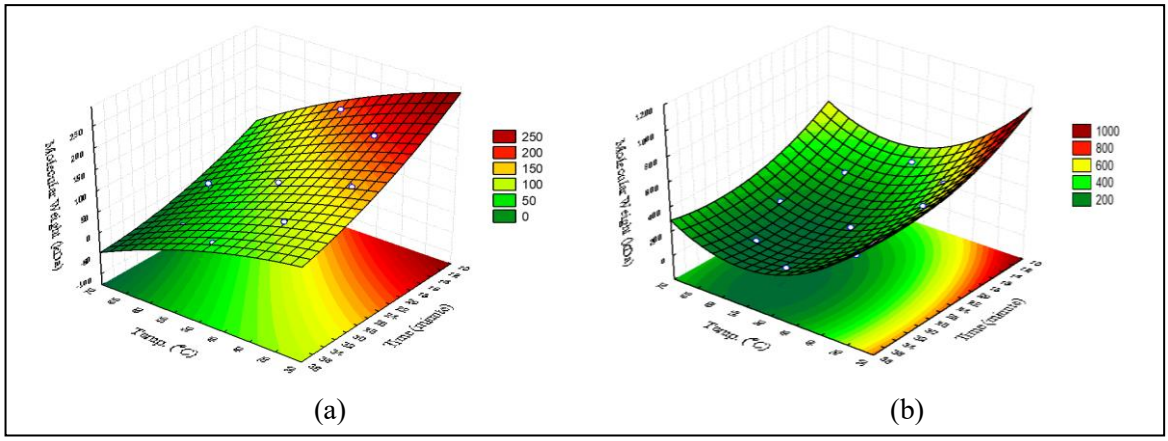

Fig. 2. Response Surface (a) pH 3 and (b) pH 6

The presence of a concave surface indicates that an optimal combination of temperature and time exists for achieving a minimum molecular weight. As the temperature and time parameters move away from the center of the concave toward the edges of the graph, the molecular weight increases. The color scale indicates a broad molecular weight range, approximately 200 to 1000 kDa.

3.5. Chemical Structure Analysis

FTIR analysis aims to determine the chemical compound content and provide information about the chemical bond structure in κ-carrageenan. Based on the FTIR analysis results [34], [35], several peaks were found around wavenumbers 1230-1270 cm^{-1}, which represent the absorptions of sulfate ester groups. Wavenumbers at 840-850 cm^{-1} indicate the presence of D-galactose-4-sulfate groups, and absorptions at wavenumbers 928-933 cm^{-1} are associated with absorptions of 3,6-anhydro-D-galactose groups. Glycosidic bonds are absorbed at wavenumbers 1040-1080 cm^{-1}. The wavenumber range and functional groups of κ-carrageenan are presented in Table 6.

Table 6. Wavenumber Spectrum of κ-carrageenan FTIR

Functional Groups	Wave Number (cm^{-1})	Absorbance pada pH 3	
		Before	*After*
O-H	3600-3000	0.3570	0.2852
C-H	3000-2800	0.1250	0.1445
C≡C	2260-2240	0.0206	0.0753
Sulfate ester (-S=O)	1380-1355	0.1794	0.0948
O=S=O (Asymmetric sulfate esters)	1270-1230	0.2022	0.1083
Glycosidic bond	1080-1040	0.1571	0.0932
3,6-anhydro-D-galactose	940-930	0.1191	0.0595
Galactose 4-sulfate	850-840	0.0982	0.0426

Based on the FTIR results in Fig. 3, it can be seen that the absorbance intensity of the κ-carrageenan sample before ultrasonication was higher than after ultrasonication. This is due to the hydrogen chain breaking, and then the water molecules being distributed into the OH groups [35]. A decrease in absorbance intensity occurred in the sulfate ester group (S=O) at the 1261 cm^{-1} peak, from 0.2022 to 0.1083. At the 850 cm^{-1} peak, indicating the presence of a galactose 4-sulfate (C–O–S) bond, the absorbance intensity decreased from 0.0982 to 0.0426. The peak at 929 cm^{-1}, indicating the presence of a C–O bond in 3,6-anhydro-D-galactose, experienced a decrease in absorbance intensity from 0.1191 to 0.0595. This suggests that in this study, there was no loss of sulfate groups in κ-carrageenan after ultrasonication. Sulfate groups in κ-carrageenan tend to be more stable after irradiation than iota and lambda carrageenan [36]. The glycosidic bond peak was observed at 1074 cm^{-1} before ultrasonication; however, after ultrasonication, there was a decrease in intensity at wavenumbers between 1080 and 1040 cm-1. This proves that bond cleavage mainly occurs at the α (1-3) and β (1-4) glycosidic bonds [37], [38].

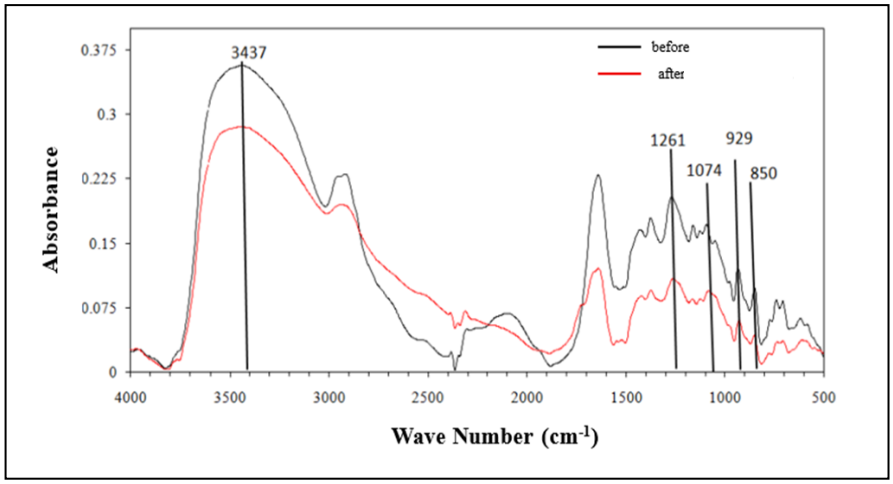

Fig. 3. FTIR spectrum of κ-carrageenan

In contrast, the sulfate group absorption band at 1250-845 cm^{-1} was relatively stable and did not experience significant changes. This indicates that ultrasonic depolymerization primarily attacks the weaker glycosidic bonds. At the same time, the sulfate group remains because the C–O–S bond in sulfate is stronger and less susceptible to attack by ultrasonic radicals. This finding is consistent with previous studies that reported ultrasonic degradation tends to damage the main chain of polysaccharides [16], [39], while substituent groups, such as sulfate, are relatively more stable. The stability of the sulfate group is crucial because the bioactive properties of κ-carrageenan, such as antiviral and anticoagulant activities, are significantly influenced by the degree of sulfation. Thus, ultrasonic depolymerization produces low-molecular-weight oligosaccharides while retaining the sulfate groups essential for their biological activity.

4. Conclusion

This study demonstrated that the ultrasonic-assisted depolymerization of κ-carrageenan is significantly influenced by pH, temperature, and time, with pH being the most significant parameter. Acidic conditions (pH 3) accelerated chain cleavage, resulting in a greater reduction in molecular weight compared to pH 6. Furthermore, increases in temperature and time enhanced degradation. The RSM-based regression model (CCD) successfully captured the individual, interaction, and quadratic effects of all variables, with R^2 values exceeding 0.96 at both pH levels, confirming its predictive reliability. FTIR analysis supported these findings by indicating that depolymerization mainly occurred at α(1→3) and β(1→4) glycosidic bonds. At the same time, sulfate ester groups remained intact—an essential feature for preserving the biological activity of κ-carrageenan. Overall, the results demonstrate that ultrasound can efficiently produce low-molecular-mass κ-carrageenan without compromising its functional sulfate groups. This work enhances the mechanistic understanding of process parameters in ultrasonic depolymerization. It highlights its potential as an eco-friendly method for producing bioactive oligosaccharides for use in functional foods, pharmaceuticals, and biomedical applications. Future studies should relate the optimized conditions to specific biological activity assays to better direct the application of low-molecular-mass κ-carrageenan in therapeutic and health-related products.

Acknowledgment

We want to thank the Department of Chemical Engineering, Faculty of Engineering, Universitas Pendidikan Muhammadiyah Sorong, for its support of this research activity.

References

[1] L. V. Abad, H. Kudo, S. Saiki, N. Nagasawa, M. Tamada, H. Fu, Y. Muroya, M. Lin, Y. Katsumura, L. S. Relleve, C.T. Aranilla, and A. M. Delarosa, "Radiolysis studies of aqueous κ-carrageenan," Nucl. Instrum. Methods Phys. Res. Sect. B Beam Interact. Mater. At., vol. 268, no. 10, pp. 1607–1612, May 2010, doi: 10.1016/j.nimb.2010.02.006.

[2] V. Y. Thien, W. T. L. Yong, A. Anton, and G. J. W. L. Chin, "A multiplex PCR method for rapid identification of commercially important seaweeds Kappaphycus alvarezii, Kappaphycus striatus and Eucheuma denticulatum (Rhodophyta, Solieriaceae)," Reg. Stud. Mar. Sci., vol. 40, pp. 101499, Nov 2020, doi: 10.1016/j.rsma.2020.101499.

[3] R. Azanza, "Eucheuma," CABI Compendium, 2023. https://doi.org/10.1079/cabicompendium.102037.

[4] C. S. Vairappan, "Seasonal occurrences of epiphytic algae on the commercially cultivated red alga kappaphycus alvarezii (solieriaceae, gigartinales, rhodophyta)," J. Appl. Phycol., vol. 18, pp. 611–617, Jul 2006, doi: 10.1007/s10811-006-9062-6.

[5] Y. Li., N. Liu, X. Wang, X. Tang, L. Zhang, M. D. N. Meinita, G. Wang, H. Yin, Y. Jin, H. Wang, C. Liu, S. Chi, T. Liu, and J. Zhang, "Comparative genomics and systematics of betaphycus, eucheuma, and kappaphycus (solieriaceae: rhodophyta) based on mitochondrial genome," J. Appl. Phycol., vol. 30, no. 6, pp. 3435–3443, Dec 2018, doi: 10.1007/s10811-018-1450-1.

[6] V. L. Campo, D. F. Kawano, D. B. da Silva Jr, and I. Carvalho, "Carrageenans: biological properties, chemical modifications and structural analysis–A review," Carbohydr. Polym., vol. 77, no. 2, pp. 167–180, Jun 2009, doi: 10.1016/j.carbpol.2009.01.020.

[7] R. Rupert, K. F. Rodrigues, V. Y. Thien, and W. T. L. Yong, "Carrageenan from kappaphycus alvarezii (Rhodophyta, Solieriaceae): Metabolism, structure, production, and application," Front. Plant Sci., vol. 13, pp. 859635, May 2022, doi: 10.3389/fpls.2022.859635.

[8] M. Haijin, J. Xiaolu, and G. Huashi, "A κ-carrageenan derived oligosaccharide prepared by enzymatic degradation containing anti-tumor activity," J. Appl. Phycol., vol. 15, no. 4, pp. 297–303, Jul 2003, doi: 10.1023/A:1025103530534.

[9] T. Yamada, A. Ogamo, T. Saito, H. Uchiyama, and Y. Nakagawa, "Preparation of O-acylated low-molecular-weight carrageenans with potent anti-HIV activity and low anticoagulant effect," Carbohydr. Polym., vol. 41, no. 2, pp. 115–120, Feb 2000, doi: 10.1016/S0144-8617(99)00083-1.

[10] Y.-H. Chiu, Y.-L. Chan, L.-W. Tsai, T.-L. Li, and C.-J. Wu, "Prevention of human enterovirus 71 infection by kappa carrageenan," Antiviral Res., vol. 95, no. 2, pp. 128–134, May 2012, doi: 10.1016/j.antiviral.2012.05.009.

[11] F. R. F. Silva, C. M. P. G. Dore, C. T. Marques, M. S. Nascimento, N. M. B. Benevides, H. A. O. Rocha, S. F. Chavante, and E. L. Leite, "Anticoagulant activity, paw edema and pleurisy induced carrageenan: Action of major types of commercial carrageenans," Carbohydr. Polym., vol. 79, no. 1, pp. 26–33, Jan 2010, doi: 10.1016/j.carbpol.2009.07.010.

[12] L. A. R. de Souza, C. M. P. G. Dore, A. J. G. Castro, T. C. G. de Azevedo, M. T. B. de Oliveira, M. d. F. V. Moura, N. M. B. Benevides, and E. L. Leite, "Galactans from the red seaweed Amansia multifida and their effects on inflammation, angiogenesis, coagulation and cell viability," Biomed. Prev. Nutr., vol. 2, no. 3, pp. 154–162, Jul 2012, doi: 10.1016/j.bionut.2012.03.007.

[13] I. Wijesekara, R. Pangestuti, and S.-K. Kim, "Biological activities and potential health benefits of sulfated polysaccharides derived from marine algae," Carbohydr. Polym., vol. 84, no. 1, pp. 14–21, Feb 2011, doi: 10.1016/j.carbpol.2010.10.062.

[14] B. Stephanie, D. Eric, F. M. Sophie, B. Christian, and G. Yu, "Carrageenan from Solieria chordalis (Gigartinales): Structural analysis and immunological activities of the low molecular weight fractions," Carbohydr. Polym., vol. 81, no. 2, pp. 448–460, Jun 2010, doi: 10.1016/j.carbpol.2010.02.046.

[15] V. H. Pomin, "Structural and functional insights into sulfated galactans: a systematic review," Glycoconj. J., vol. 27, no. 1, pp. 1–12, Jan 2010, doi: 10.1007/s10719-009-9251-z.

[16] L. Zhang, X. Ye, T. Ding, X. Sun, Y. Xu, and D. Liu, "Ultrasound effects on the degradation kinetics, structure and rheological properties of apple pectin," Ultrason. Sonochem., vol. 20, no. 1, pp. 222–231, Jan 2013, doi: 10.1016/j.ultsonch.2012.07.021.

[17] R. Ratnawati, A. Prasetyaningrum, and D. H. Wardhani, "Kinetics and thermodynamics of ultrasound-assisted depolymerization of κ-carrageenan," Bull. Chem. React. Eng. Catal., vol. 11, no. 1, pp. 48–58, Apr 2016, doi: 10.9767/bcrec.11.1.415.48-58.

[18] R. Ratnawati and N. Indriyani, "Kinetics and thermodynamics study of ultrasound-assisted depolymerization of k-Carrageenan in acidic solution," Bull. Chem. React. Eng. Catal., vol. 15, no. 1, pp. 280–289, Apr 2020, doi: 10.9767/bcrec.15.1.6738.280-289.

[19] K. Tarman, M. W. Zuhair, Uju, and R. F. Pari, "Ultrasound-assisted depolymerization of carrageenan from kappaphycus alvarezii hydrolized by a marine fungus," IOP Conf. Ser. Earth Environ. Sci., vol. 1137, no. 1, pp. 012048, Jan 2023, doi: 10.1088/1755-1315/1137/1/012048.

[20] R. H. Myers, D. C. Montgomery, G. G. Vining, C. M. Borror, and S. M. Kowalski, "Response surface methodology: a retrospective and literature survey," J. Qual. Technol., vol. 36, no. 1, pp. 53–77, Jan 2004, doi: 10.1080/00224065.2004.11980252.

[21] Ö. Türkşen, "Analysis of response surface model parameters with bayesian approach and fuzzy approach," Int. J. Uncertain. Fuzziness Knowl.-Based Syst., vol. 24, no. 01, pp. 109–122, Feb 2016, doi: 10.1142/S0218488516500069.

[22] I. Veza, M. Spraggon, I. R. Fattah, dan M. Idris, "Response surface methodology (RSM) for optimizing engine performance and emissions fueled with biofuel: Review of RSM for sustainability energy transition," Results Eng., vol. 18, pp. 101213, Jun 2023, doi: 10.1016/j.rineng.2023.101213.

[23] [J. Yanchun and G. Bing, "Exploring the progressive optimization technique within response surface methodology," dalam 2024 IEEE 4th International Conference on Information Technology, Big Data and Artificial Intelligence (ICIBA), Chongqing, China: IEEE, pp. 1370–1374, Des 2024, doi: 10.1109/ICIBA62489.2024.10868680.

[24] J. Oh, "A modified class of composite designs for the response model approach with noise factors," Int. J. Ind. Eng. Theory Appl. Pract., vol. 30, no. 1, Feb 2023, doi: 10.23055/ijietap.2023.30.1.8311.

[25] H. M. Ibrahim, W. M. W. Yusoff, A. A. Hamid, R. M. Illias, O. Hassan, and O. Omar, "Optimization of medium for the production of β-cyclodextrin glucanotransferase using central composite design (CCD)," Process Biochem., vol. 40, no. 2, pp. 753–758, Feb 2005, doi: 10.1016/j.procbio.2004.01.042.

[26] E. R. V. Almeida, A. S. Melo, A. S. Lima, V. A. Lemos, G. S. Oliveira, C. F. Cletche, A. S. Souza, and M. A. Bezerra, "A review of the use of central composite design in the optimization of procedures aiming at food chemical analysis," Food Chem., vol. 480, pp. 143849, Jul 2025, doi: 10.1016/j.foodchem.2025.143849.

[27] A. Asghar, A. A. Abdul Raman, and W. M. A. W. Daud, "A Comparison of central composite design and taguchi method for optimizing fenton process," Sci. World J., vol. 2014, pp. 1–14, Aug 2014, doi: 10.1155/2014/869120.

[28] H. J. Vreeman, T. H. M. Snoeren, and T. A. J. Payens, "Physicochemical investigation of k -carrageenan in the random state," Biopolymers, vol. 19, no. 7, pp. 1357–1374, Jul 1980, doi: 10.1002/bip.1980.360190711.

[29] C. Rochas, M. Rinaudo, and S. Landry, "Role of the molecular weight on the mechanical properties of kappa carrageenan gels," Carbohydr. Polym., vol. 12, no. 3, pp. 255–266, 1990, doi: 10.1016/0144-8617(90)90067-3.

[30] S. Beg and Z. Rahman, "Central composite designs and their applications in pharmaceutical product development," in Design of Experiments for Pharmaceutical Product Development, S. Beg, Ed., Singapore: Springer Singapore, 2021, pp. 63–76, doi: 10.1007/978-981-33-4717-5_6.

[31] Y. S. Yoon, G. H. Goh, J. H. Song, S. H. Oh, I. H. Cho, S. Y. Kang, C. H. Park, S. H. Lee, "Method for producing biofuels via hydrolysis of seaweed extract using heterogeneous catalyst," WO Appl., vol. 2010098585, pp. A2, 2010.

[32] H.-Y. Yen and M.-H. Yang, "The ultrasonic degradation of polyacrylamide solution," Polym. Test., vol. 22, no. 2, pp. 129–131, Apr 2003, doi: 10.1016/S0142-9418(02)00054-5.

[33] D. E. Myslabodski, D. Stancioff, and R. A. Heckert, "Effect of acid hydrolysis on the molecular weight of kappa carrageenan by GPC-LS," Carbohydr. Polym., vol. 31, no. 1–2, pp. 83–92, Sep 1996, doi: 10.1016/S0144-8617(96)00054-9.

[34] E. Gómez-Ordóñez and P. Rupérez, "FTIR-ATR spectroscopy as a tool for polysaccharide identification in edible brown and red seaweeds," Food Hydrocoll., vol. 25, no. 6, pp. 1514–1520, Aug 2011, doi: 10.1016/j.foodhyd.2011.02.009.

[35] H. Agougui, M. Jabli, and H. Majdoub, "Synthesis, characterization of hydroxyapatite-lambda carrageenan, and evaluation of its performance for the adsorption of methylene blue from aqueous suspension," J. Appl. Polym. Sci., vol. 134, no. 40, pp. 45385, Okt 2017, doi: 10.1002/app.45385.

[36] N. Shrgawi, I. J. Shamsudin, H. Hanibah, S. A. Mohd Noor, and N. Kasim, "Purification on kappa carrageenan by re-precipitation technique," Solid State Phenom., vol. 317, pp. 327–332, May 2021, doi: 10.4028/www.scientific.net/SSP.317.327.

[37] P. Volery, R. Besson, and C. Schaffer-Lequart, "Characterization of commercial carrageenans by Fourier transform infrared spectroscopy using single-reflection attenuated total reflection," J. Agric. Food Chem., vol. 52, no. 25, pp. 7457–7463, Dec 2004, doi: 10.1021/jf040229o.

[38] C. Lii, C.-H. Chen, A.-I. Yeh, dan V. M.-F. Lai, "Preliminary study on the degradation kinetics of agarose and carrageenans by ultrasound," Food Hydrocoll., vol. 13, no. 6, pp. 477–481, Nov 1999, doi: 10.1016/S0268-005X(99)00031-4.

[39] J.-K. Yan, J.-J. Pei, H.-L. Ma, dan Z.-B. Wang, "Effects of ultrasound on molecular properties, structure, chain conformation and degradation kinetics of carboxylic curdlan," Carbohydr. Polym., vol. 121, hlm. 64–70, May 2015, doi: 10.1016/j.carbpol.2014.11.066.